BULLETIN OF THE POLISH ACADEMY OF SCIENCES
TECHNICAL SCIENCES, Vol. 69(2), 2021, Article number: e136743
DOI: 10.24425/bpasts.2021.136743

Ultra-fast hybrid systems for protecting direct current circuits with high magnetic energy

Marek BARTOSIK, Piotr BORKOWSKI*, and Franciszek WÓJCIK

Lodz University of Technology, Department of Electrical Apparatus (DEA TUL), 116 Zeromskiego Street, 90-924 Lodz, Poland

Abstract. The article presents a new generation of ultra-fast hybrid switching systems (USH) for reliable, ultra-fast protection of various medium and low voltage DC systems (MVDC and LVDC). The DC switch-off takes place in a vacuum chamber (VC) cooperating with a semiconductor module using current commutation of natural or forced type. Against the background of the current state of science and technology, the paper depicts the basic scopes of USH applications and their particular suitability for operation in high magnetic energy DC circuits. In the case of DC system failures, this magnetic energy should be dissipated outside the system as soon as possible. Usually, magnetic blow-out switches (MBOS) with relatively low operating speed are used for this purpose. The article describes the theoretical basis and principles of construction of two types of novel USH systems: a direct current switching system (DCSS) and a direct current ultra-fast hybrid modular switch (DCU-HM). The DCSS family is designed for quench protection of superconducting electromagnets' coils in all areas of application. The DCU-HM family is designed for the protection of all systems or vehicles of DC electrical traction and for related industrial applications. The conducted comparative analysis of the effectiveness of USH with respect to MBOS shows clear technical advantages of the new generation switching systems over MBOS. List of abbreviations used in the article is provided at the end.

Key words: DC; direct current; superconducting coils; quench; electromagnets protection; DC switches; ultra-fast switches; hybrid switches; vacuum switches; DC electric traction.

1. Introduction

The DC ultra-fast shutdown technology started to be developed after 1930 in Sweden (ASEA). It has focused mainly on the high DC voltage (HVDC) range used in long-distance transmission systems or AC coupling lines. The types of DC circuit-breakers used at that time were assessed as lacking in effectiveness. These were usually circuit-breakers with sufficiently large breaking capacity, but with long total break times[1] and current limitation coefficients[2] $C_o \approx 1$. Effective mitigation of the harmful effects of short circuit currents requires effective mitigation of these currents, i.e. breakers as fast as possible with the lowest possible C_o. Similar needs exist for medium DC voltages (MVDC) used in DC1 (3 kV) and DC2 (1.5 kV) systems of railway traction and in some propulsion or electrothermal devices, as well as in low voltage systems (LVDC, up to 1250 V) used in all types of city or mining electric traction and numerous industrial systems (converters, propulsions, etc.) [1–5].

For the last 20 years, a very large number of publications has focused on vacuum, hybrid or solid state switches with many different topologies, designed for networks and power systems, mainly in the HVDC range (e.g. [6–8]). This goes beyond the scope of this paper.

2. Current state-of-the-art of DC shutdown

For the protection of MVDC and LVDC systems, magnetic blow-out switches (MBOS) with an arc in atmospheric air are usually used. The devices have been known for over 120 years and they are being continuously improved.

The MBOS switches off short-circuit currents by an increase in arc resistance R_a in the ceramic extinguishing chamber, which absorbs the energy of the power source and magnetic energy of the circuit. When the arc resistance increases sufficiently to meet the following condition: $R_a > U_s/i(t) - R_s$ (where U_s is the supply voltage, $i(t)$ – current course, and R_s – short circuit resistance), the current derivative di/dt is always negative until the current reaches zero. Therefore, in DC circuits, when the magnetic energy increases, the switching life of MBOS decreases.

The greatest magnetic energies, of even up to 10 MJ, are found in superconductive electromagnets (SE). This exceeds the capabilities of extinguishing chambers used in MBOS. In emergency situations, to dissipate these energies a technique of bypassing the main switch with a dump resistor RD is used. After opening the switch and extinguishing the arc, RD takes over the SE supply current. The magnetic energy of SE is converted in the RD into heat released to the environment. In this case, the high speed of the switch operation, i.e. the shortest possible total break time T_b, has a great impact on reducing the harmful effects of SE's failure [9].

The search for new technical solutions for DC circuit-breakers, much faster than MBOS, is stimulated by the increasing needs in rail transport in DC1 and DC2 systems. This is caused by the tendency to increase the acceleration and speed of the

[1] Total break-time: $T_b = t_t - t_0$, where t_t – tripping instant, t_0 – arc extinction instant in main contact.
[2] Current limitation coefficient $C_o = i_o/I_u$, where i_o – limited current, I_u – steady short circuit current.

*e-mail: piotr.borkowski@p.lodz.pl

Manuscript submitted 2020-12-13, revised 2021-02-06, initially accepted for publication 2021-02-13, published in April 2021

rolling stock, the introduction of semiconductor devices into traction drives (e.g. for pulse start-up and braking with energy recovery and for the introduction of DC-powered AC drives via converters), and the dissemination of energy storage systems. It results in the increase of the substation supply voltage (on the AC side), in the increase of substation and vehicle motor power, and in the use of power amplification systems to limit voltage drops. The above-mentioned factors cause the increase of short-circuit power and steepness of the short-circuit current change on the DC side [10].

New technical solutions of ultra-fast DC circuit-breakers (U DCCB), designed for rail transport, can be adapted to work in a variety of SE applications.

These requirements can hardly be met by the MBOS, which has too low short-circuit shutdown rate and too high Joule integral value (I^2t), especially for effective protection of semiconductor systems. This is one of the development barriers for railway traction.

There is no universal classification covering all DC switches. Traction switches are divided into 3 categories in terms of operating speed: S, H, V, with total break time $T_b \leq 30$; 20; 4 ms (respectively) [11]. MBOS can be classified into categories of S or H, i.e. it can achieve current limitation factors of $C_{0S} \geq 0.95$ or $C_{0H} \geq 0.7$. Hence, the current limitation efficiency in typical circuits with a time constant $\tau > 10$ ms is practically none (for S) or negligible (for H). The circuit-breakers in category V must have values $C_{0V} \leq 0.3$. This can be easily achieved with ultra-fast vacuum or hybrid switches. MBOS systems have reached the peak of their technical capabilities in all typical applications, which is due to their principle of operation.

A multilateral research and implementation program, covering the issues of vacuum U DCCBs, has been carried out by the Authors in the Department of Electrical Apparatus at Lodz University of Technology since 1980. The theoretical basis developed made it possible to create and implement a new generation of ultra-fast DC vacuum circuit breakers, designed for substations and railway traction vehicles in the DC1 system (a total of 16 sizes with different voltages and currents) [10]. Fast technical progress in the field of railway combined with new needs and requirements created the necessity to retrofit the switches designed for DC1 and DC2 systems. After appropriate adaptation, new designs of circuit breakers have been developed and used among others for ultra-fast protection of SE against quench[3] effects.

In each of these areas of application, there are different system, environmental and technical requirements. Therefore, ultra-fast hybrid systems have two design variants: DCSS for the area of superconductive electromagnets and DCU-HM for the area of electric traction. Both variants use the same theoretical basis and related principles of operation of the hybrid switch-off system. It must be emphasized that only those principles of operation and topologies, out of 17 types of DC circuit breakers classified in [4], whose suitability for MVDC and LVDC has been verified experimentally [12–16], were analyzed in the USH implementation program.

3. Theoretical basis and principles of USH operation

3.1. Ultra-fast opening of USH. Ultra-fast opening of USH has been achieved due to development of a special vacuum switch with fixed position under the force of return spring, opened by means of one-way induction-dynamic drive IDD[4] [1, 2, 5, 7, 17] of high power (ring driving disc electrodynamically rejected from the coil powered by the impulse of high-current from the energy storage), kept in open state by a quick lock. Current pulses in the coil have the high first semi-wave amplitude and frequency. Changes in coil magnetic field induce current in the disc. Interaction of both currents generates the impulse of electrodynamic driving force.

The IDD construction diagram is shown in Fig. 1. Moving part of the switch is a tilt-less, straight line mechanism with a vacuum chamber galvanically separated from other components. It is rigidly coupled with the moving contact and the disc, which enables direct transmission of the disc motion onto the chamber's moving contact. This is an instant commencement of contact opening upon equalization of increasing driving force of the disc and the return force. USH uses selected series-produced vacuum chambers for MV AC circuit-breakers.

It is required that the coil and the vacuum chamber be suspended as rigidly as possible on the support structure and that the drive disc be rigidly connected to the vacuum chamber, in order to shorten the opening time of the vacuum interrupter, in which its mechanical structure is responsible for the largest part of the delay. This is directly justified by all three of Newton's laws of dynamics, with respect to the interactions of the individual IDD components, causing deformations and axial elastic oscillations.

IDD current pulses, generated by an oscillatory discharge of the capacitor charged to U_{C0} voltage by coil 9, usually have first halfwave amplitude > 1 kA and time up to 300 μs. Change in the magnetic field of a coil induces current in the toroidal disc, whose cross-section is rectangular. The interaction of currents generates a pulse of electrodynamic driving force F_D repelling the drive, which is coupled with the rest of the components of the moving body (see elements 5–9 in Fig. 9c), from the coil.

3.2. Vacuum interrupters for USH application. Industrial AC vacuum chambers can be used in USH for DC if they meet certain requirements [14, 18, 19]. The prerequisite is that only the diffusion form of the vacuum arc is present in the vacuum interrupter. The properties of the diffusion arc are essential for the use of vacuum interrupters for ultra-fast DC switching off by USH. There must be no constricted arc. Only vacuum chambers with contact-generating axial magnetic field (AMF) may be used. This is shown in Fig. 2.

[3] Quench: accidental local decay of superconductivity in SE coil. The resistance area quickly spreads in the coil due to Joule heat generated by great coil magnetic energy. This causes significant damage.

[4] So-called Thomson drive.

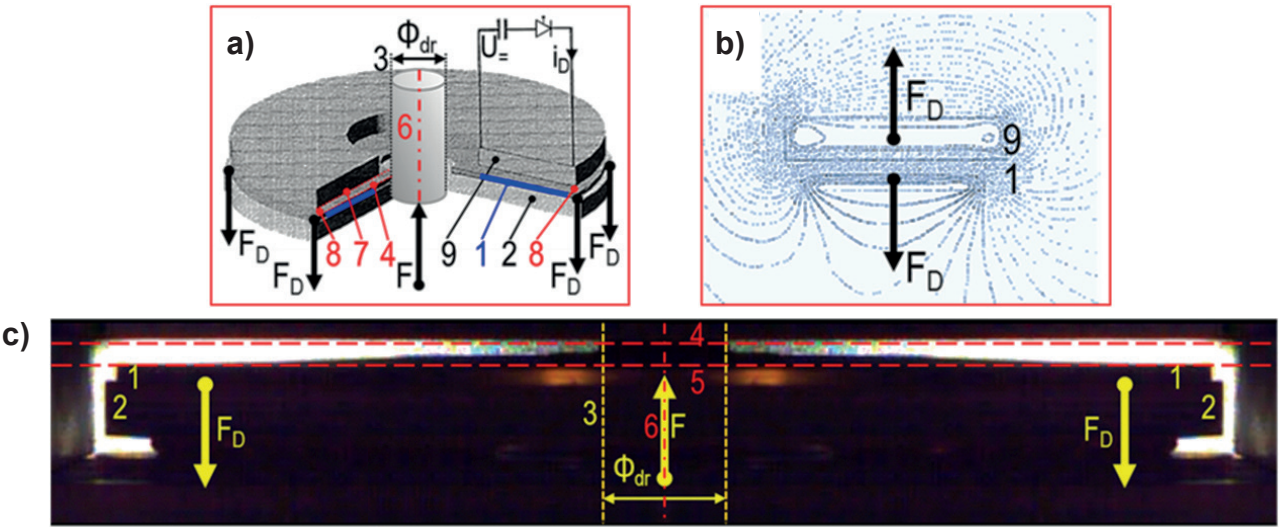

Fig. 1. IDD's coil and disc in the initial movement stage: a) IDD model in currentless mode, b) spatial electromagnetic field distribution in the area of the coil's maximum current i_D and generated propulsion force, c) chosen frame from the movement examination taken with the high-speed camera (20 000 fps), with a special backlight for better exposure of deformation of the disc system. 1 – copper disc, 2 – disc body, 3 – a piece of drive linkage diameter Φ_{dr}, 4 – line of the external upper edge and of the whole disc area before switching on the current, 5 – line of the disc edge in the moment of the maximum current, 6 – symmetry axis of the drive, 7 – line of the lower area of the coil's edge, 8 – operational gap between the disc and the coil, 9 – equivalent active cross-section of the coil. F – spring force (contact pressure), F_D – drive force (which opens the vacuum interrupter)

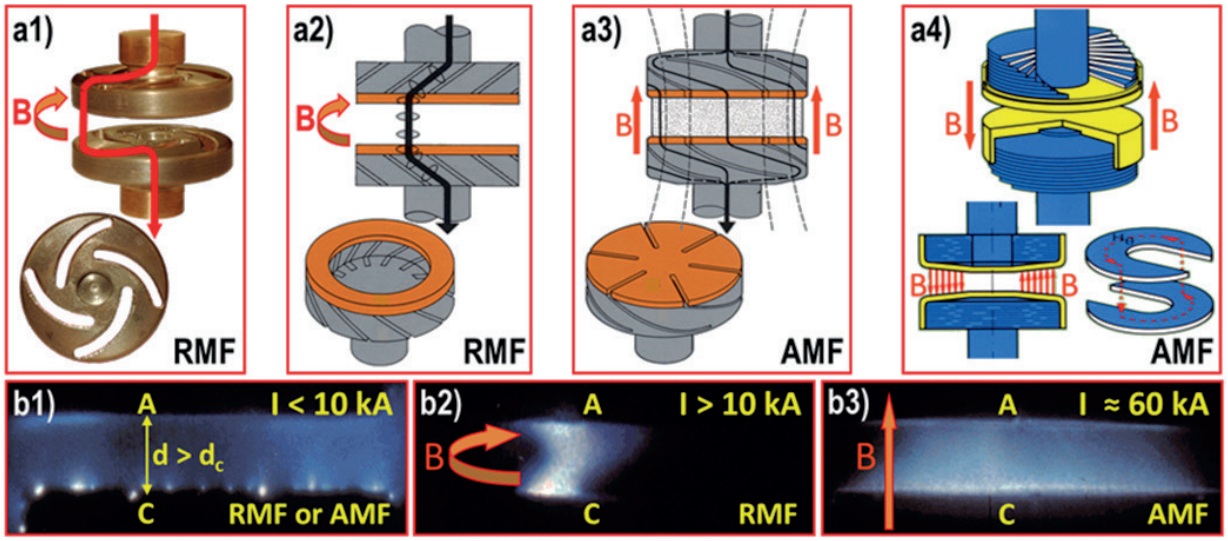

Fig. 2. Effect of magnetic field on the arc in a vacuum. a) Examples of contacts generating radial magnetic field RMF or axial magnetic field AMF: a1) spiral contact, a2) crown contact, a3) coil contact, a4) ferro contact (field shaped by multi-layer horseshoe-shaped steel inserts placed under the contact tips). b) Forms of the vacuum arc: b1) diffusion arc at currents below 10 kA limit, both at RMF and AMF, b2) constricted arc with active anode at currents greater than the 10 kA limit at RMF, b3) diffusion arc with passive anode at currents much higher than 10 kA limit at AMF. B – magnetic flux density, A – anode, C – cathode, d – contacts distance, d_c – critical distance of contacts (Phot. acc. to [20], own description)

There is a large safety margin for USH under real operating conditions, while using a vacuum chamber with AMF for AC circuit-breakers with contact material without low melting components (typically CuCr alloys are used), at experimentally verified limit current $i \approx 60$ kA and $d > d_c = 0.3$ mm. With typical geometric dimensions of the contact system, after the current is reduced to zero and the diffusion arc is extinguished, the initial parameters of the post-arc plasma are subcritical and the mean free path of atoms is greater than the distance between the contacts d.

Under these conditions, after current zero, the recovery strength increases rapidly to the static electrical strength of the cold vacuum gap, $u_{vd} = K \cdot d$, where K denotes static flashover intensity in the vacuum. The K value is high and it depends on the contact material, e.g. for Cu, flat contacts $K \approx 80$ kV/mm. If the current reaches zero for d in the range of 0.3–0.5 mm,

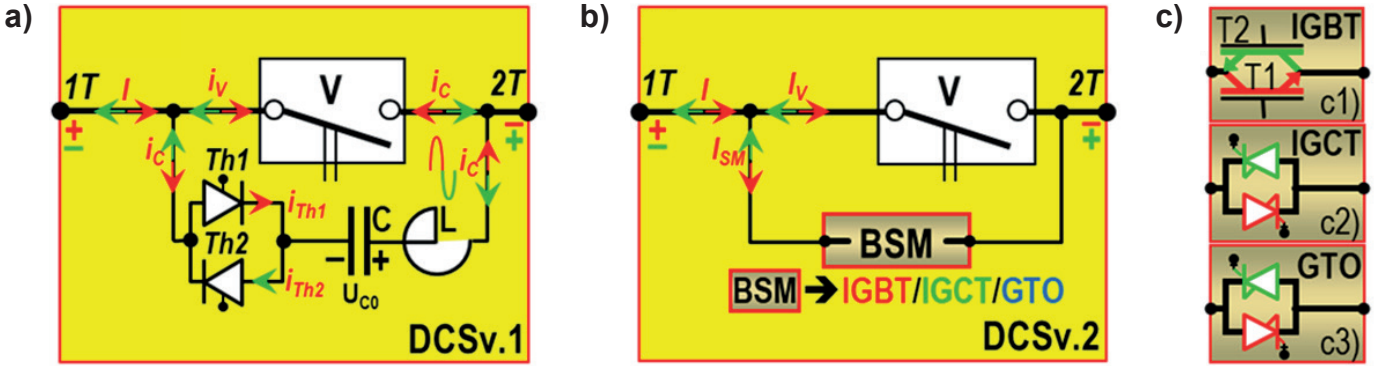

Fig. 3. Ultra-fast DCS switches: a) v.1 version with forced commutation, b) v.2 version with natural commutation. V – vacuum interrupter; 1T, 2T – main terminals; Th1, Th2 – thyristors; C – commutation capacitor, L – air-core reactor. BSM – bidirectional semiconductor module; c) BSM types: c1) – IGBT, c2) – IGCT, c3) – GTO. Currents: I – main c. (any direction); i_V – arc c., i_C – counter-current; i_{Th1}, i_{Th2} – thyristor c., i_{SM} – BSM current. U_{C0} – initial voltage of C capacitor. Note: the C capacitor is charged: from an inverter supplied with auxiliary voltage (for DCSS v.1), or from the overhead contact line (for DCU-HMv.1)

the breakdown voltage is in the range of 24–40 kV. Hence, arc reignition is impossible.

The presence of a constricted arc is excluded, as the active anode is a strong source of metal vapor for the contact gap. This greatly reduces the K value. If the direct current goes to zero with high steepness, it may not be switched off. At diffusion arc in AMF, assuming a surge protection level of approx. 10 kV, a reduction of current to zero at $d \geq d_c = 0.3$ mm may be safely realized. To minimize the total break time T_b, the highest opening speed v_o of the vacuum chamber (provided by the producer) must be assumed.

3.3. Quench phenomenon. Superconducting coils supplying all types of electromagnets in accelerators are usually made of Rutherford multi-wire cables, spliced from multiple filament wires, in order to reduce the number and inductance of coils. Despite of the very rigid structure of the superconducting coil (due to compression in dedicated steel flanges), in order to eliminate any movements of cable wires, Lorentz forces affect the wires and may locally exceed friction forces, causing micro movements of wires and instantaneous release of sufficient heat to cause local loss of superconductivity.

Resistance area is generated at random, at the unknown location of the coil, and propagates rapidly due to conduction of heat generated by Joule losses in the resistance area, including magnetic energy dissipation. This is accompanied by overvoltage on the coil, much higher than the supply voltage. This enables quench detection. Under typical conditions, quench propagates transversally (coil to coil) within ca. 10 ms and the electromagnet undergoes damage due to local overheating or voltage breakdown. The issue of shortening the coil current off time and superconducting coil energy discharge is essential to reduce the damage caused by the quench. There are no overvoltages, overloads and short circuits in the power supply circuits of superconducting coils, so this does not apply to anti-quench protection systems. The high magnetic energies of the coils are transferred in an ultra-fast manner to dump resistors, and converted to heat (see Section 2).

3.4. Operating principles of USH. Depending on the purpose of the USH system, two variants of ultra-fast DC hybrid switches (DCS), with different operating principles, are used alternatively: DCS v.1, with forced commutation, and DCS v.2, with natural commutation. Diagrams of both DCS variants are shown in Fig. 3.

DCS v.1 with forced commutation (Fig. 3a) is an ultra-fast, unpolarized DC hybrid switch with parallel hybrid topology of vacuum-thyristor type that brings the direct current to zero in the vacuum with a counter-current pulse from an additional source switched with thyristor module.

The countercurrent is sinusoidal. Its source is capacitor C charged to voltage U_{C0}. C is unloaded due to switching on the thyristors. Th1 and Th2 thyristors are switched on sequentially. The current in a vacuum chamber is the difference between the main current and the countercurrent. Depending on the direction of the main current, it can be reduced to zero as a result of a single (during the first counter-current half-wave, see Fig. 4d) or a double (during the second counter-current half-wave, see Fig. 4e) commutation.

DCS v.2 with natural commutation is an ultra-fast, unpolarized DC hybrid switch with parallel hybrid topology of vacuum-semiconductor type. It brings the direct current to zero in the vacuum with the difference between the arc voltage $u_a = 10$–27 V (18–21 V for Cu contact) of the diffusion arc in the vacuum chamber and the conducting voltage $u_{SM} \approx 2$ V of the parallel connected bidirectional semiconductor module (BSM), activated for a short time. The BSM can be an anti-parallel combination of IGBT transistors, or IGCT thyristors (possibly GTO). In each BSM, both transistors or thyristors are controlled simultaneously. The current-compatible element takes over its conduction.

After the diffusion arc has been extinguished in an ultra-fast manner, vacuum chamber V becomes an isolation gap. This changes the configuration of the external circuit. A naturally disappearing transition state appears, depending on the parameters of the circuit. For each range of USH applications, the course of phenomena in this state is different.

4. Detailed specification of USH application areas

4.1. Area of superconductive electromagnets. DCSS family for anti-quench protection. Coils of superconducting electromagnets for:

- elementary particle accelerators,
- tokamaks and stellarators for nuclear fusion,
- accelerators in the industry, medicine (cancer treatment, imaging techniques, NMR, manufacturing processes and new materials, food preservation), in the army,
- traction (MAGLEV) and magnetic cushion bearings,
- plasma generators, energy storage, etc.

General conditions of DCSS operation: conduction and deactivation of direct current of a given value. There are no short circuits or overloads. There are no switching overvoltages. Overcurrent releases and surge arresters are not required. An ultra-fast shutdown is required (shutdown as short as possible). Both DCS v.1 and v.2 variants are used.

4.2. Area of electric traction. DCU-HM family for substations and vehicles protection.

- DC1 railway traction system (U = 3 kV).
- DC2 railway traction system (U = 1.5 kV).
- Urban traction systems, LV (U $\leq$ 1 kV), trams, trolley buses, buses etc.
- Mining traction systems, LV (U $\leq$ 0.6 kV).
- Industrial applications, LV (U = 0.25–1.25 kV) and related.

DCU-HM types for railway traction:

- P type circuit breakers (stationary), for substations.
- Vehicle circuit breakers (mobile): PZ type for combined trains, L for locomotives and others. Roof, deck or sub-deck versions are possible.

General DCU-HM operating conditions: direct current on and off of any value possible in a given traction system at the highest supply voltage, as well as limiting overvoltages. There are operating, overload and short-circuit currents. There are two-sided switching overvoltages (external – network, or atmospheric and internal – receiver). Overcurrent releases and surge arresters are necessary. Ultra-fast short-circuit breaking (shortest possible total break time) and energy recuperation are required. Both DCS v.1 and v.2 variants are used. None of them must operate due to typical driving disturbances [21].

5. DCSS as a modern protection system

A simplified scheme of powering the superconducting magnet coil, containing the energy extraction system (EES), is shown in Fig. 4a, while the simulated waveforms of voltages and currents presented in Fig. 4b–4e illustrate the ultra-fast operation of DCSS v.1 and v.2.

Each DCSS v.1 or v.2 is unpolarized and redundant, i.e. it consists of two identical DCS v.1 or v.2 (respectively), marked A and B in Fig. 4a. Due to the natural dispersion of phenomena, one of the DCS (A or B) works first (in random order). The second one opens currentlessly. So, the ultrafast DCSS and DCS shutdown sequences are the same. Ultra-fast DCSS in all required conditions may constitute a replacement for the MBOS used so far in EES.

The external OFF command or QDS quench detection signal immediately activates commands 1–3 (Fig. 4a), causing the DCPS to be turned off, BC to be turned on, and switches A and B to be opened at the same time (at instant t_{50} in Fig. 4b–4e). After T_o opening time, at instant t_{cs}, contacts of the vacuum chamber V split and move away at the set speed. When the contact distance d increases above d_c (see Section 3.2), at instant t_{6o}, the command ON starts the ultra-fast shutdown sequence. This sequence is slightly different for DCS v.1 and v.2.

The SS v.1 unified shutdown algorithm sequence is very simple for forced commutation (green color in Fig. 3a). It contains only three consecutive control signals separated by strictly defined two delay times (T_{d1}, T_{d2} in Fig. 5.c):

$$\mathbf{OFF_{DCSS}}(t_{5o}) \blacktriangleright \mathbf{T_{d1}}(T_{5o-6o}) \blacktriangleright \mathbf{ON_{Th1}}(t_{6o}) \blacktriangleright \blacktriangleright \mathbf{T_{d2}}(T_{5o-7o}) \blacktriangleright \mathbf{ON_{Th2}}(t_{7o}). \tag{1}$$

The delay times can be adjusted to synchronize the operation of both DCS v.1, cooperating in series in DCSS v.1. Depending on the direction of the main current, it can be reduced to zero at instant t_{ae} as a result of a single or double commutation (Fig. 4d, 4e); (see also Section 3.4). After instant t_{ae}, RD resistor quickly takes over the main current and starts discharging energy from SM.

The SS v.2 shutdown algorithm sequence for DCS v.2 is even simpler than SS v.1. It consists of only two successive control signals separated by a specified delay time T_{5o-6o}:

$$\mathbf{OFF_{DCS}}(t_{5o}) \blacktriangleright T_{5o-6o} \blacktriangleright \mathbf{ON_{T1,T2}}(t_{6o}) \sqcap \sqcap (t_{7o})\mathbf{OFF_{T1,T2}}, \tag{2}$$

where the ON $\sqcap$ $OFF_{T1,T2}$ is the command for IGBT modules, in the form of voltage single pulse of duration T_{6o-7o} (Fig. 4b, 4c).

As a result of the auto-adaptation of the IGBT module to the direction of the main current I, first V/T commutation between V and T1 or T2 is performed spontaneously by one of the transistors T1 or T2, having the direction of conduction in accordance with the direction of the main current. After instant t_{7o}, resistor RD quickly takes over the main current and starts discharging energy from SM (Fig. 4b, 4c). The coil current flows in the SM-BC-RD loop (Fig. 4a), until the magnetic energy is completely lost as a result of conversion into heat in the RD (see Section 2).

6. DCS operation

Detailed block diagrams of DCS v.1/v.2, following the principles of operation shown in Fig. 3, and unified DCS v.1 and DCS v.2 ON/OFF cycle are presented in Fig. 5. DCS v.1 and the DCS v.2 have different principles of operation and construction,

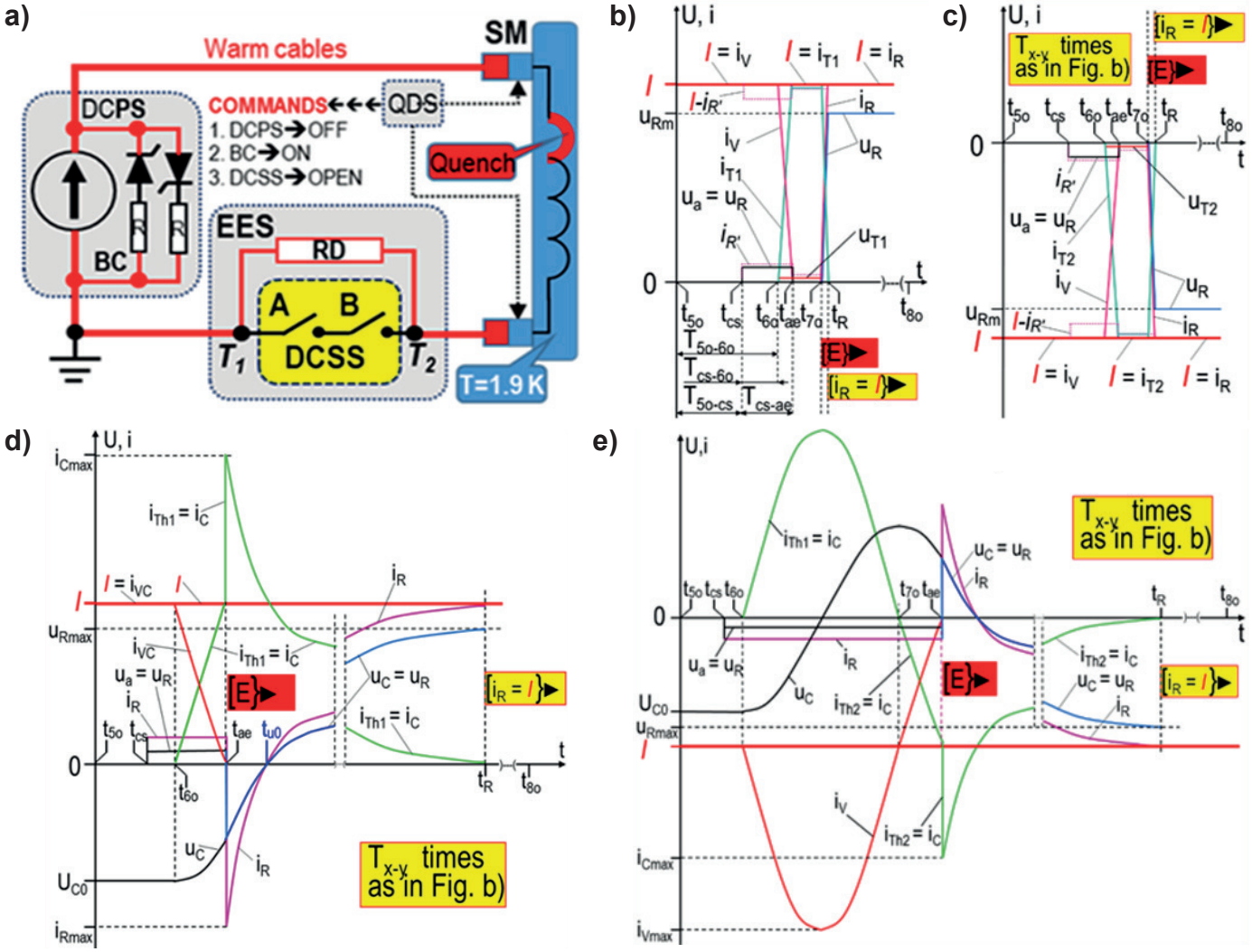

Fig. 4. General principle of ultra-fast protection of superconducting coils against quench effects. (a) Simplified scheme for superconducting coil power supply, equipped with an energy extraction system containing ultra-fast DCSS. Currents and voltages when DC is switched off: with natural commutation – (b) with positive current polarity, (c) with opposite current polarity, for DCS v.2 shown in Fig. 3b; (d) with forced commutation – with consistent current and counter-current direction (i.e. $i_V = I - i_C$, single commutation); (e) with opposite current and counter-current direction (i.e. $i_V = I + i_C$, double commutation), for DCS v.1 shown in Fig. 3a. DCPS – direct current power supply, SM – superconducting magnet coil, BC – bypass circuit, QDS – quench detection system, EES – energy extraction system, DCSS – redundant switching system (two identical ultra-fast DCS v.1 or v.2 switches (A and B), RD – dump resistor (for coil energy discharge); T1, T2 – terminals

but they are functionally fully equivalent. Each of them must be able to independently and reliably switch off the main current of the superconducting coil. Therefore, each DCS is equipped with a similar control system, with slight differences in software and control elements of thyristors or transistors. DCS v.1 becomes v.2 when the ThU and CCU modules are replaced by an IGBTM module (Fig. 5a).

Full switching cycle (ON/OFF) of DCSS consists of four sequences: preparation sequence, switching on sequence, main current conduction sequence and ultra-fast shutdown sequence (intentional or as a result of a quench). Three of them shown in Fig. 5b (preparation, switching on and current conduction sequences) are identical for DCS v.1 and DCS v.2. Small differences between DCS v.1 (Fig. 5c) and v.2 (Fig. 5d) exist during shutdown sequence only.

During the DCS preparation sequence (time $T_{1c–2c}$), auxiliary voltage is switched on at instant t_{1c} and signal S1 starts self-control of all monitored parameters R1–Rn. DCS automatically sets itself in the open position and goes into standby mode, sending the standby signal S2 (at instant t_{2c}), and awaits further commands. During the DCS switching on sequence (time $T_{3c–4c}$), signal S3 at instant t_{3c} is the command to close DCS. Hence, lock LS is opened, vacuum switch VCU is closed, and DCS enters the standby mode, sending closed state signal S4 (at instant t_{4c}). The DCS conduction sequence has an indefinite time $T_{4c–5o}$. The current is externally switched on at the moment of t_{ON} and conducted until instant t_{5o}, when the switch off command is sent.

Ultra-fast shutdown sequence in time $T_{d1} = T_{5o–6o}$ (Fig. 5c, 5d) is the same for DCS v.1 and v.2. After receiving at instant

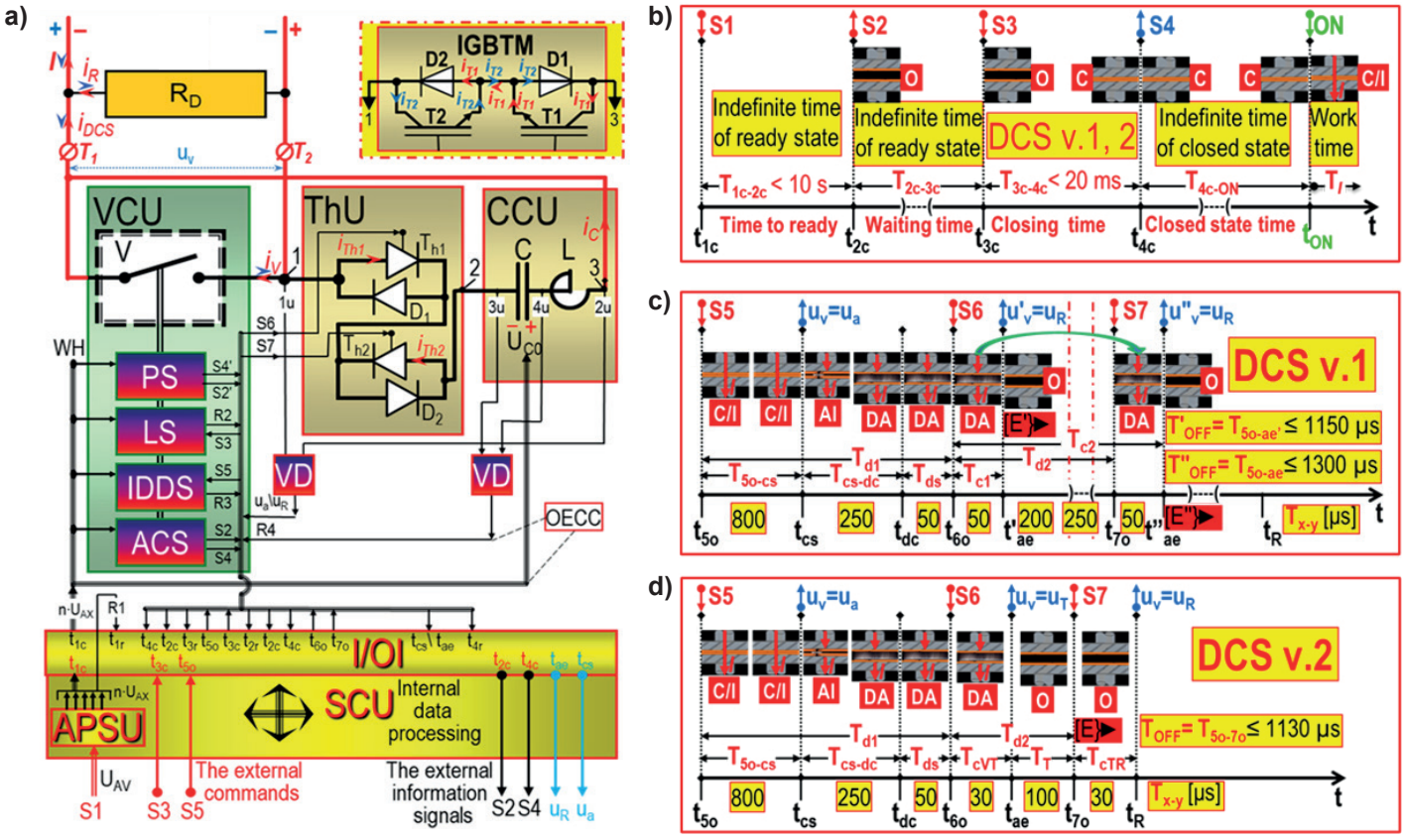

Fig. 5. Unified DCS v.1 and DCS v.2 ON/OFF cycle for both directions of main current *I* and for the circuit features shown in Fig. 2–4. a) Block diagram of DCS v.1/v.2 for any polarity of main current I. b) Sequence of switching on the circuit (identical for DCS v.1 and DCS v.2). Unified shutdown sequence, its elements and times: c) for DCS v.1, of thyristor-vacuum type with forced commutation; d) for DCS v.2, of transistor-vacuum type with natural commutation. Pictograms showing the states of contact of vacuum chamber V (see also VC in Fig. 9b): O – open, C – closed (no current), C/I – closed (current flow), AI – arc ignition, DA – diffuse arc; [E}► – beginning of energy discharge. **The markings in Fig. a:** VCU – vacuum contact unit: V – vacuum interrupter, PS – position sensor, LS – lock set, IDDS – inductive-dynamic drive set, ACS – auxiliary contact set (instead of ACS, a second PS can be used); ThU – thyristor unit; CCU – counter-current unit; VD – voltage dividers, 1u, 2u, 3u, 4u – voltage measurement points; T_1, T_2 – terminals; 1, 2 – connection points; SCU – control unit of DCS switch with input/output interface I/OI; OECC – optical or electrical control connections; WH – wiring harness; APSU – auxiliary power supply unit. **Signals:** S1 – sequence start (as a result of auxiliary voltage: U_{AV} → ON and $n \cdot U_{AX}$ ON, see Fig. a and Fig. b); S2 – ready state of DCS; S3 – command to close DCS; S4 – DCS closed state; S5 – opening command (OFF DCS s.), S6 – command to turn on thyristor Th_1 (ON Th_1 s.), S7 – command to turn on thyristor Th_2 (ON Th_2 s.). **The markings in Fig. d: Signals:** S5 – as previously, S6 – command to simultaneously turn on transistor T1 and T2 (ON T_{1+2} s.); S7 – command to simultaneously turn off transistor T1 and T2 (OFF T_{1+2} s.)

t_{5o}, the DCS opening command S5 (external OFF command or quench signal (see Section 5, Fig. 4)), the shutdown sequence SS v.1 or SS v.2 starts (see Section 5, Eq. (1) or Eq. (2)). The contact of vacuum interrupter V opens ultrafast over total opening time T_{5o-cs}. The contact distance increases above critical distance $d_c = 0.3$ mm (see Section 3.2) in the set delay time T_{cs-6o}. Then, it becomes possible to switch off the current and extinguish the diffusion arc in interrupter V at instant t_{ae}, according to SS v.1 with a single (Fig. 4d) or double (Fig. 4.e) commutation, or according to SS v.2 (Fig. 4b, 4c) commutation. The full commutation time T_{60-R} includes the first commutation between the interrupter V and the semiconductor module Th or T (in time T_{60-ae}), the second commutation between module Th or T and resistor RD (in time T_{ae-R}) and the start of energy dump from the superconducting coil. The second commutation is a self-disappearing transient state determined by the RLC parameters, without practical meaning for energy dump. Next the DCS stays in the open position and automatically goes into standby mode, sending standby signal S2 at the instant t_{8o} to EES (i.e. informational signal of opening and readiness state, see Fig. 5b, see also Fig. 4). In this state DCS awaits further commands.

The parameters of the ultra-fast shutdown sequence shown in Fig. 5c, 5d are an illustration of the DCS v.1 and v.2 dynamic capabilities (sec. 5, Eq. (1) or Eq. (2)).

Time values T_{x-y} in Fig. 5b and 5c are given for DCS 2000 A. They may differ slightly for other DCS rated currents. For example, for DCS 600 A, total break time values are, respectively, $T'_{OFF} \leq 650$ µs $\approx T_{OFF}$, $T''_{OFF} \leq 800$ µs. They do not exceed 1.6 ms for the current range of up to 4–5 kA, i.e. the limit of the possibility of building a unipolar DCS.

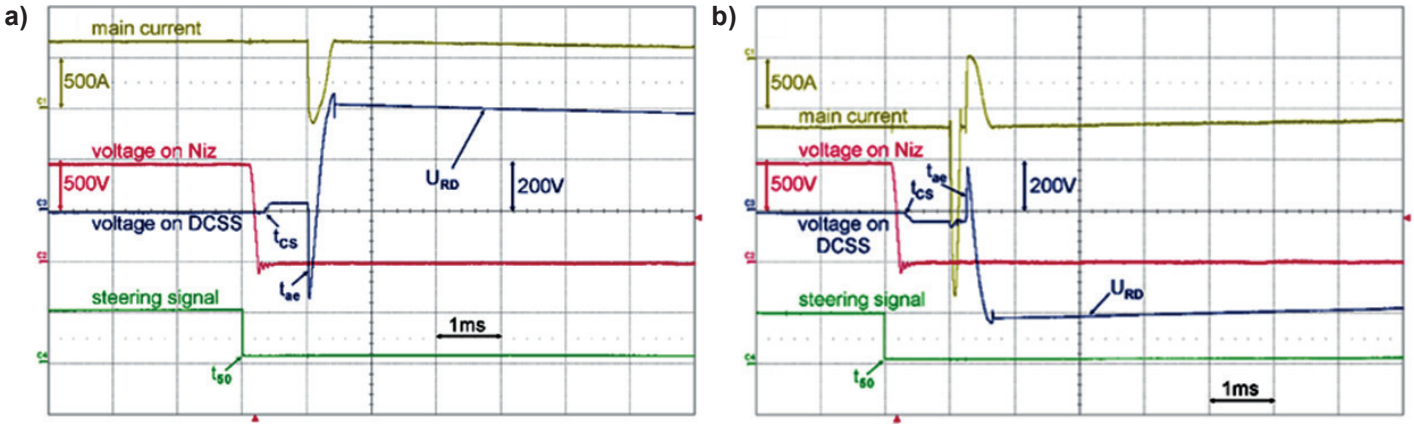

Fig. 6. Oscillograms of the main current of 600 A commutation between DCS v.1 and dump resistor RD with forced commutation: a) single, b) double (Section 3.4 and Figs. 4d, 4e)

The increase in T_{OFF} time is the result of increasing, together with the current, the mass of the moving contact of vacuum chamber V and the drive components connected to it (see Fig. 5a). This increases opening time T_{5o-cs} (Figs. 5c, 5d), which is the largest component of T_{OFF} time. In the case of higher currents, in the absence of suitable vacuum chambers, two or more DCS connected in parallel and operating simultaneously should be used.

The excellent dynamic properties of DCSS allow for an approximately 40-fold reduction in the total break time (below 2 ms) in relation to outdated MBOS. This is crucial for limiting the quench effects.

Sample measurements conducted during commutation of the main current of 600 A by the dump resistor for DCS v.1 for single (see Fig. 4d) and double (see Fig. 4e) commutation are illustrated in Fig. 6a and Fig. 6b, respectively. By analogy, Fig. 7 presents similar oscillograms obtained for DCS v.2. Furthermore, the example of current commutation of 2000 A obtained experimentally for DCS v.1 is shown in Fig. 8. Even though the time base is different on oscillograms presented in Fig. 6 and Fig. 8, the similarities and differences in the switching process can be noticed, as discussed above.

DCS v.1 with forced commutation is useful within the whole current and voltage range. DCS v.2 with natural commutation is useful in the lower range.

The main parameters of each of the DCSS/DCS v.1 and v.2 variants differ. For the needs of CERN, DCSS with the following parameters were developed and implemented for unit production:

$$\text{DCSS v.1: } U = 1500 \text{ V; } I = 600, 2000, 13\,000 \text{ [A]}. \quad (3)$$

Planned ➔ 24 000 A.

$$\text{DCSS v.2: } U = 1500 \text{ V; } I = 600 \text{ A}. \quad (4)$$

The DCSS family implementation program has been carried out for the European Organization for Nuclear Research CERN. All manufactured DCSS (600 A and 2000 A) were installed at CERN in 2019 for quench protection of superconducting electromagnets operating in LHC (Large Hadron Collider) systems.

A new technique of ultrafast commutation of the current between the DCSS/DCS and dump resistor RD has been experimentally verified. It improves the effectiveness and reliability

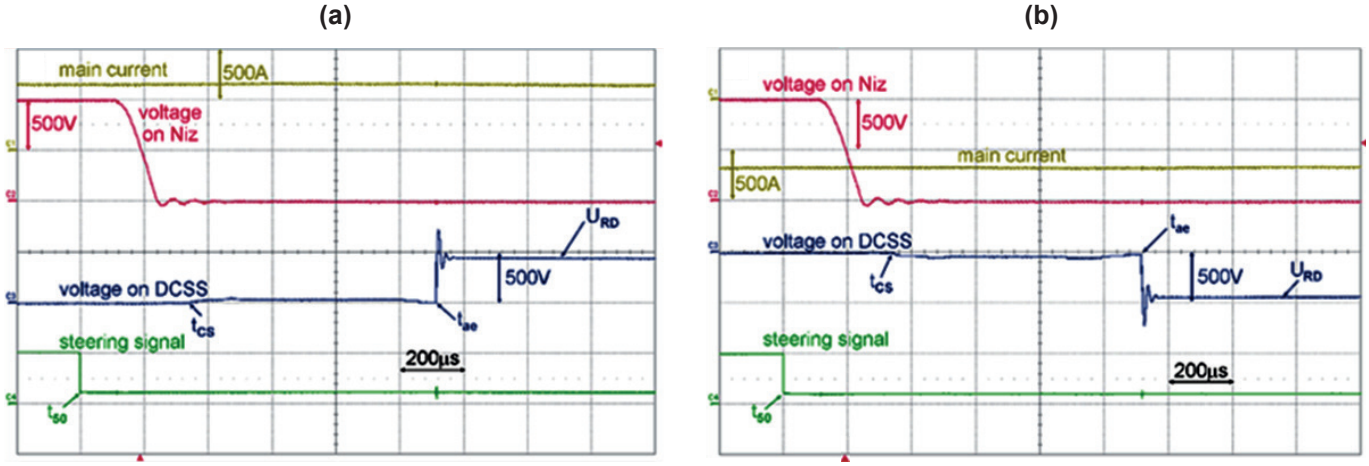

Fig. 7. Oscillograms of the main current of 600 A commutation between DCS v.2 and dump resistor RD with forced commutation: a) single, b) double (Section 3.4 and Figs. 4d, 4e)

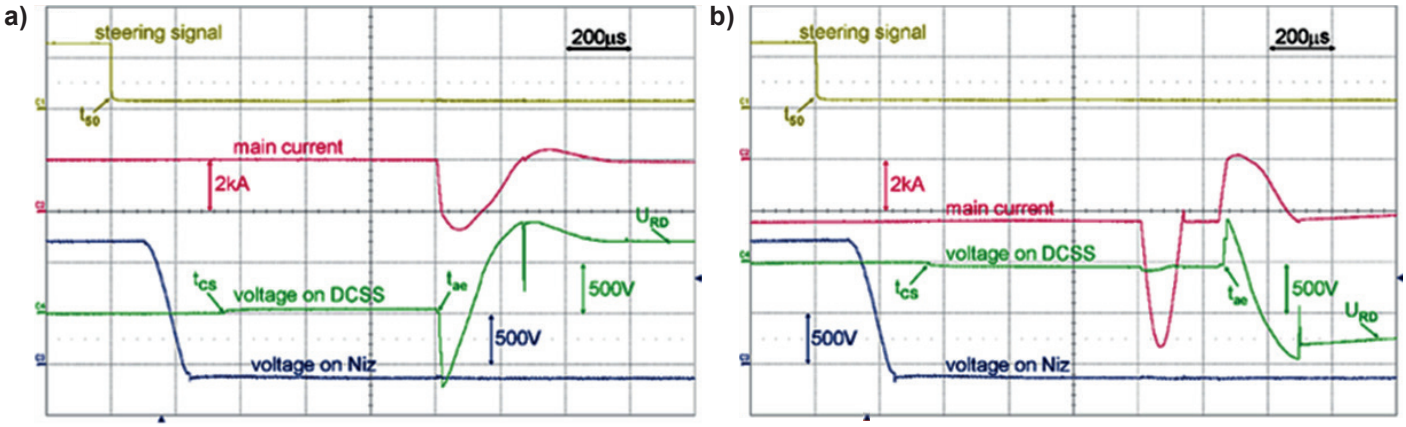

Fig. 8. Oscillograms of the main current of 2000 A commutation between DCS v.1 and dump resistor RD with forced commutation: a) single, b) double (Section 3.4 and Figs. 4d, 4e)

of anti-quench protection. The development potential of DCSS is high because they can be useful in all fields of application of superconducting electromagnets described in Section 4.1. Selected examples from the DCSS family photo-documentation are shown in Fig. 9.

Sample oscillograms taken during switching off of the current of 13 000 A by DCSS13 v.1 shown in Fig. 9d are presented in Fig. 10. Meanwhile, Fig. 10a and Fig. 10b depict the obtained waveforms with forced commutation: a) single, b) double (Section 3.4 and Figs. 4d, 4e).

7. DCU-HM as modern protection system for DC1 and DC2 railway traction systems

Similar to DCSS, ultra-fast DCU-HM in all the required conditions may constitute a replacement for the MBOS used so far in electric traction. The origin of the work on the DCU-HM family is described in Section 2. DCU-HM are designed for railway traction vehicles used in both DC1 and DC2 systems, and also in other DC LV systems. They have an optimized operating principle and new breaker topology.

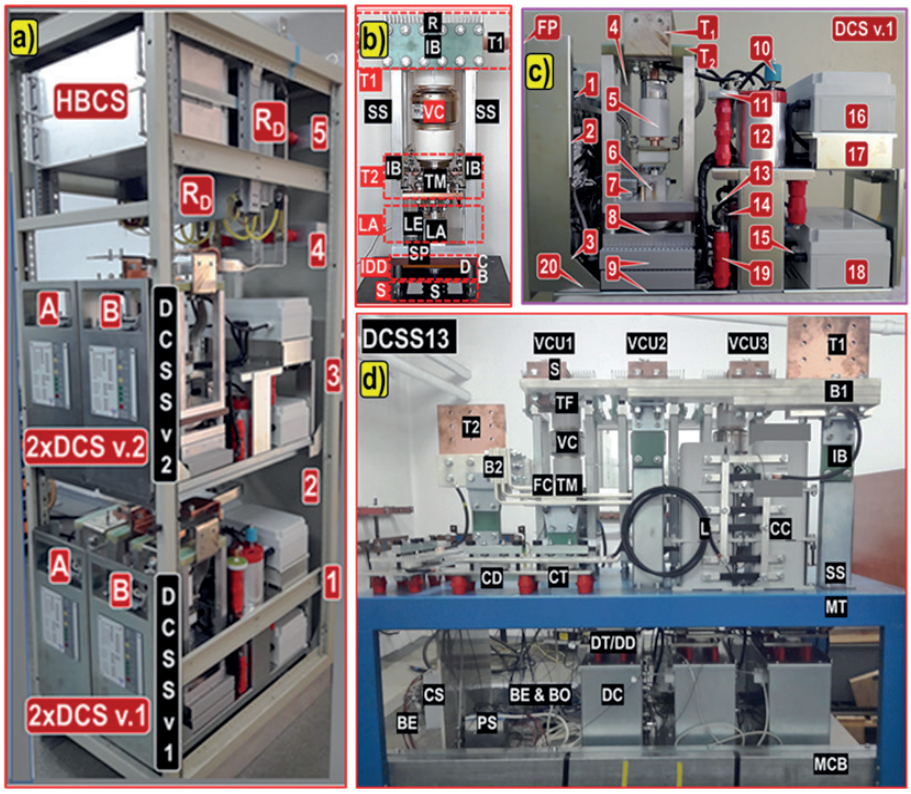

Fig. 9. Selected examples from the DCSS family photo-documentation

a) DCSS v.1 and v.2, 600 A systems mounted in the Eurorack: 1 – DCSS v.1 compartment; 2 – compartment of DCSS v.1 main circuit flexible connections; 3 – DCSS v.2 compartment; 4 – compartment of DCSS v.2 main circuit flexible connections; 5 – compartment of HBCS master controller of EES and RD dump resistors; A, B – individual DCS switches (see Fig. 4.a).

b) Ultra-fast vacuum contact unit (VCU), main assemblies and components. Terminals of VC vacuum interrupter: T1 – fixed terminal cooled by R heat sink, T2 – movable terminal with flexible connections; LA – lock assembly, and LE – lock engine; IDD – inductive-dynamic drive: C – coil, B – bumper, D – disc; S – spring set, IB – insulation bracket, SP – supporting plate, SS – supporting structure.

c) DCS v.1 switch overview and its subassemblies, for DCSS v.1, 2000 A system, panoramic left side view: T1, T2 – main terminals, FP – front panel; 1 – terminal strip, 2 – local control panel, 3 – power supplies of lock release electromagnet, 4 – vacuum contact unit VCU, 5 – vacuum interrupter VC, 6 – lock assembly LA, 7 – position sensor PS, 8 – inductive-dynamic drive set IDD, 9 – contact spring set S, 10 – filter capacitor, 11 – commutation reactor L, 12 – commutation capacitor (CC), 13 – IDD coil diode, 14 – drive capacitor, 15 – drive release thyristor, 16 – converter for charging the commutation capacitor 12; 17 – controller of thyristors, 18 – converter for charging the drive capacitor 14; 19 – insulators, 20 – elements of mounting cage. **Note:** all symbols in brackets – see Fig. b or Fig. d.

d) DCSS13 v.1 (3 kV, 13000 A). VCU1, 2, 3 – ultra-fast vacuum contact units working in parallel; B1, 2 – main high current busbars, BE – electric bundle, BO – fiber optic bundle, CC – counter-current capacitor, CD – counter-current backward diodes, CS – control system, CT – counter-current thyristors, DC – drive capacitors, DD – drive diodes, DT – drive thyristors, FC – flexible connections, IB – insulating brackets, L – air-core reactor, MCB – main construction base, MT – mounting table, PS – power supply; S – measuring shunts, SS – supporting structure, T1, 2 – terminals, VC – vacuum interrupters. **Note:** VCU1, 2 and 3 have the same design.

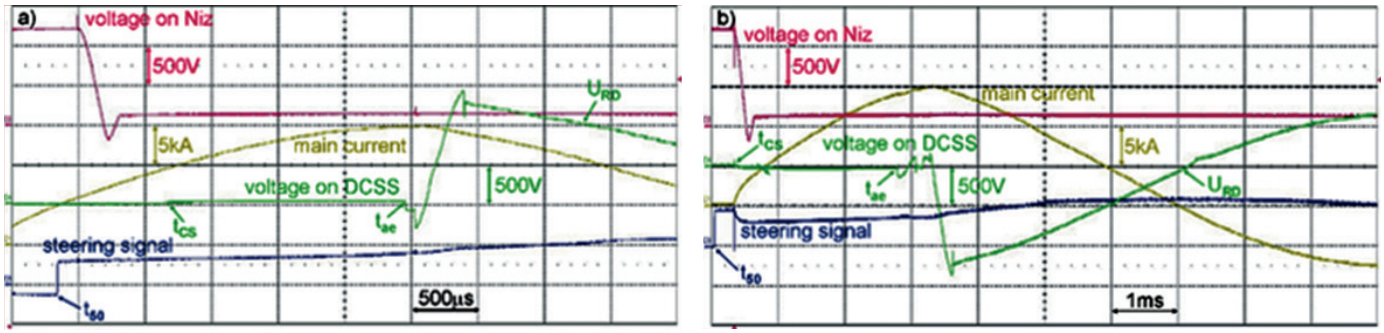

Fig. 10. Oscillograms of the main current of 13 000 A commutation to dump resistor RD obtained for DCSS13 v.1 with forced commutation: a) single, b) double (Section 3.4 and Figs. 4d, 4e)

The latest technical conditions are taken into account. The switching off of DC by natural commutation (version v.2) is only useful in the low voltage range. Switching DC off by forced commutation (version v.1), i.e. by counter-current (see Section 3.4, Fig. 3a, DCS v.1), makes the devices applicable for the whole range of traction voltages. In DC1 and DC2 systems (the MVDC range), a hybrid circuit-breaker DCU-HM v.1 with a topology shown in Fig. 11 is used. An algorithm of switching

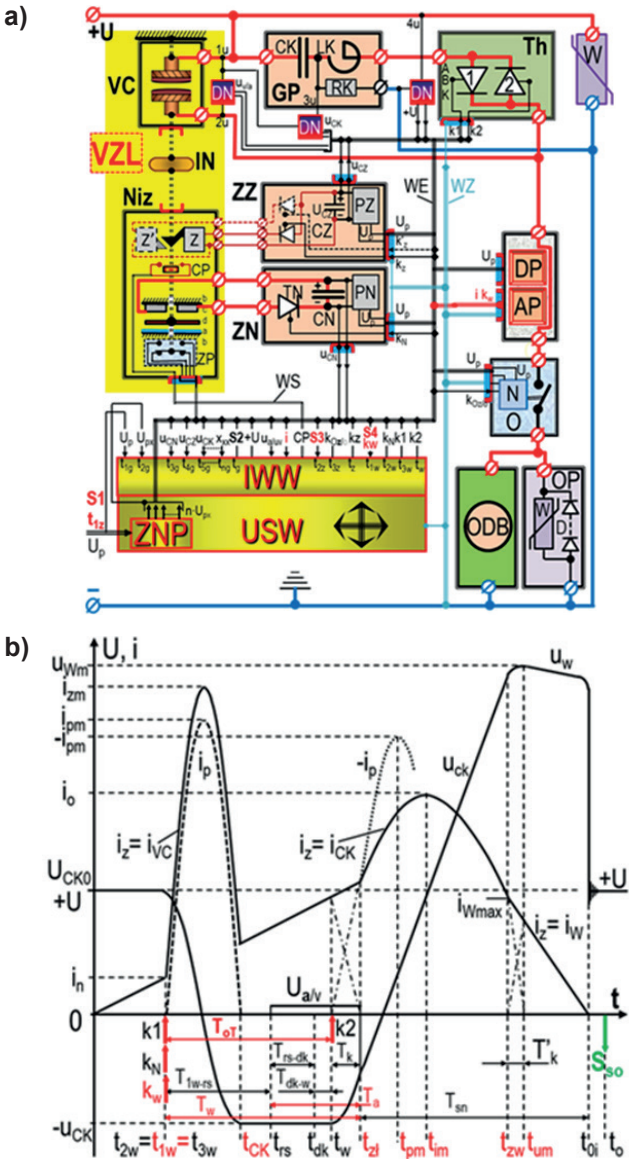

Fig. 11. a) Main circuit diagram of the new DCU-HM v.1 circuit-breaker, illustrating the basic principles of construction and operation. b) Stylized currents and voltages illustrating the ultra-fast switching off sequence (see Fig. 5c). **Symbols in Fig. 11a:** VZL – vacuum switch: VC – main vacuum chamber, P – drive rod; IN – drive insulator; Niz – inductive-dynamic drive (b – base, c – coil, d – drive, a – bumper); F_z – return force, F_n – drive force; Z – lock (main; alternatively, a second auxiliary/release lock Z'); CP – optical position sensor, ZP – auxiliary switch, WS – optical fiber harness conducting contact position signals; ZN – drive power supply: CN – drive capacitor, TN – drive thyristor, PN – drive converter; ZZ – lock power supply: PZ – lock converter, CZ – lock capacitor, TZ – lock thyristors; GP – counter-current generator: CK – commutation capacitor, LK – commutation choke, RK – commutation resistor; Th – main thyristor module 1 and 2: A – anode, B – gate, K – cathode; DP/AP – overcurrent relay: ss – special bus, DP – current discriminator, AP – current analyzer with ADC – analog-digital converter. O – disconnector (optional): N – disconnector drive; Surge arresters: external W (oxide varistor) and internal OP (W – as above and D – return diodes); ODB – traction vehicle receivers; DN – voltage dividers. "+" and "–" – main connection terminals. Terminal "–" effectively earthed (to rail). USW – central switch control unit: IWW – input-output interface, ZNP – auxiliary voltage supply. **Symbols in Fig. 11b: Voltages:** +U – mains v., $u_{a/v}$ – arc v. or v. on vacuum chamber VC; u_{CK} – v. on CK capacitor, U_{CK0} – initial value of u_{CK}, $-u_{CK}$ – initial value of u_{CK} after overload of CK, u_W – v. on varistor W, u_{Wm} – maximum value of u_W. **Currents:** i_z – short circuit c., i_m – maximum value of i_z, i_p – overload current of CK, i_{pm} – maximum value of i_p, $-i_p$ counter-current, $-i_{pm}$ – maximum value of $-i_p$, i_o – limited current, i_n – setting current of discriminator DP, i_{VC} – c. in VC chamber, i_{CK} – c. in CK capacitor, i_W – c. in W varistor, i_{Wm} – maximum value of i_W; ics. – internal control signals; t – time. **Moments:** t_{1w}, t_{2w}, t_{3w} – moments when an external S3 signal or an internal k_w signal (which initiates the shutdown sequence) is given to the USW, and k_N and k1 signals (Fig. b) are sent immediately, t_{CK} – m. of change of u_{CK} voltage polarization, t_{rs} – m. of VC contacts separation and arc ignition, t_{dk} – m. when critical contact distance is reached, t_w – m. of the k2 ics., $t_{zł}$ – m. of arc extinguishing, t_{pm} – m. of maximum counter-current ($-i_{pm}$ in Fig. b), t_{im} – m. of maximum main current, t_{zw} – m. of varistor W activation, t_{zk} – m. of commutation end between CK and W as well as the peak value of the switching overvoltage u_{Wm}, t_{0i} – m. of reaching zero by main current, t_o – m. of sending S_{so} signal ending the switching off sequence. **Times:** T_{1w-rs} – own time of VZŁ opening, T_a – arc time, T_{rs-dk} – time of reaching critical distance of contacts, T_{dk-w} – reserve time (safety reserve, delay k2), T_{oT} – delay time of k2; T_k, T'_k – commutation times, $T_w = T_{1w-zł}$ – break time, T_{sn} – transient state time ($\approx T_{oso} = T_{zł-to}$ – time of delay of S_{so} signal)

on sequence is practically the same as in DCS v.1 (see Section 6, Fig. 5b). A unified shutdown sequence of DCU-HM v.1 occurs during $T_{wo} = t_{1w} - t_o$. Its course is analogous to that shown in Fig. 5c (see also Section 5 and Eq. (1)). The values of individual times may vary, depending on many parameters. In the counter-current generator GP, commutation capacitor CK is charged from the overhead contact line (see Fig. 11a). The main current is always reduced to zero at instant t_o as a result of double commutation (Fig. 8b) (see also Section 3.4 and Section 5, Fig. 4e).

The ultra-fast shutdown sequence is triggered by the external control signal S3 (in Fig. 11a) under operating conditions, or an internal k_w signal from the overcurrent protection DP/AP at short circuit or overload, causing the Niz drive to be tripped, the VC chamber to be opened, thyristors Th1 and Th2 to be (successively) switched on (i.e. GP to be started), the current in the VC chamber to be reduced to zero by means of the counter-current and the arc to be extinguished. The switching overvoltages generated then are limited by varistor arresters W, with the use of reversible diodes D. The overcurrent relay DP/AP under overload conditions operates after exceeding the set threshold value of the Joule integral, calculated from the measured and analyzed current course, i.e. it operates as a typical thermal overcurrent tripping device. Such signal can also come from external overcurrent relays. Under short-circuit conditions, the DP/AP relay operates as an instantaneous tripping device that reacts to the set current. In any case, the ultra-fast shutdown sequence has the same course until the arc is extinguished.

According to the diagram shown in Fig. 11a, vacuum chamber VC and counter-current generator GP are connected in parallel. Generator GP is serially connected to a unit of thyristors Th1 and Th2, connected anti-parallelly. The GP generator circuit is a resonant circuit with very low attenuation, consisting of capacitor CK, which serves as energy storage, charged by resistor RK from the overhead line to $+U = U_0$, and the choke LK. According to the sequence shown in Fig. 11b), after starting the breaker with S3 signal (see also Section 6, Fig. 5b) and simultaneously giving the k_N command to switch on the drive and k1 to switch on the branches of thyristor Th1, the CK is oscillatively overcharged with a strong current impulse i_p of i_{pm} amplitude, in the circuit of CK–LK–Th1–VC, to the voltage $|-u_{CK}| < |U_0|$. Simultaneously, the k_N command starts the ultra-fast drive Niz opening VC.

After the critical distance of the contacts in VC is exceeded, the k2 command is issued with a slight delay, causing the branches of thyristor Th2 to switch on and resulting in oscillatory discharge of CK by a strong-current impulse $-i_p$, called the counter-current, with the amplitude $-i_{pm}$, having the opposite direction to i_z and i_p in VC. Counter-current $-i_p$ initially flows in the circuit of CK-LK-Th2-VC. The effect of the commutation of i_z and $-i_p$ currents in the VC contact is to reduce the i_z current to zero and to extinguish the diffusion arc. The contact gap in the out-of-current state immediately achieves very high electrical strength, which ends the process of ultra-fast i_z current shutdown. Then a natural, spontaneously fading transient state, depending on the circuit parameters, occurs in time T_{sn}. VC becomes an isolation break, which results in a change in the configuration of the circuit. A further CK discharge process takes place in a series-connected closed circuit:

> **terminal "+"** → CK → LK → Th2 → DP/AP → O → ODB (shorted) → terminal "–" → network with the equivalent parameters LS and RS (seen from the breaker terminals) → **terminal "+"**

Since LS and RS depend on the parameters of the power supplies in the overhead contact line substation and the unit parameters of the overhead contact line etc., they may have different values that depend on the position of the vehicle on the railway line section during a short circuit. The sum of the remaining energy in CK and the magnetic energy of the overhead contact line causes the overcharging of capacitor CK. Increase of u_{CK} with polarization according to +U causes reduction of the discharge current and increase of switching overvoltage on CK to the value of the tripping voltage u_w. W is a tripping varistor that takes over the remaining current and completely discharges the circuit energy.

The characteristic times of the ultra-fast multi-stage shutdown sequence shown in Fig. 8b are an illustration of the dynamic capabilities of DCU-HM (see also Section 5, Eq. (1) or Eq. (2)). Exemplary time values T_{x-y} for DCU-HM 3 kV, 1600 A, following the notation from Fig. 11b, are:

$T_{1w-rs} = 500$ µs, $T_ł = 1300$ µs, $T_{rs-dk} = 1200$ µs,

$T_{dk-w} = 40$ µs, $T_k = 60$ µs, $T_{oT} = 1740$ µs; $T_{sn} \geq 1$ ms.

Time interval $T_w \leq 2$ ms is the sum of the vacuum switch own time T_{1w-rs} with the value of 300–800 µs and the arc time $T_ł$ with the value of 1.2–1.7 ms. It is a design parameter of the circuit breaker only. On the other hand, time interval $T_{sn} \geq 1$ ms depends on both the parameters of the breaker and the parameters of the switched-off circuit, especially its inductance. As the value of the inductance increases, time T_{sn} rises. However, when switching off low inductance circuits with short-circuit currents of the order of 50 kA (traction circuits), this time may reach a value of approx. 1 ms, resulting in total break time of approx. 4 ms, which is the limit value for class V circuit breakers [22].

Similar to DCS (see Eq. (1)), unified shutdown sequence is very simple. It contains only two consecutive control signals separated by strictly defined delay times T_{oT} (Fig. 11b):

$$\text{OFF} \equiv \text{k1, } k_N\text{, kw } (t_{1-3w}) \blacktriangleright T_{oT} \blacktriangleright \text{k2 } (t_w). \tag{5}$$

For the needs of the DC1 system, the DCU-HM v.1 family has two base sizes with the following parameters:

$$\text{DCU-HM 3/1.6: U} = 3\text{k V; } I_{th} = 800, 1250, 1600 \text{ A}, \tag{6}$$

$$\text{DCU-HM 4/4.0: U} = 4\text{ kV; } I_{th} = 2500, 3150, 4000 \text{ A}, \tag{7}$$

where: DCU-HM 3/1.6 is designed for PZ, EZT and EW up to 5 MW; DCU-HM 4/4.0 is designed for high power locomotives (over 5 MW) or substations.

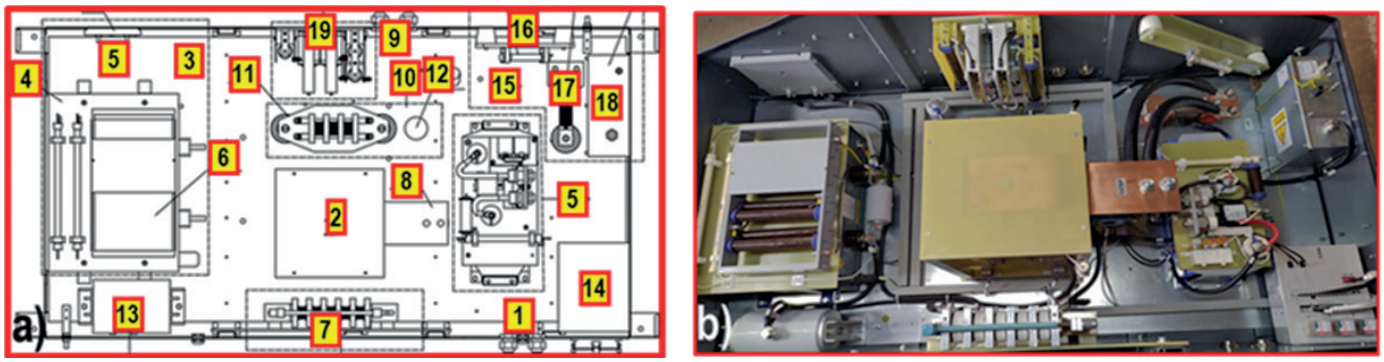

Fig. 12. Top view of the complete prototype of the DCU-HM 3/1.6 circuit breaker in the roof version. a) Design sketch with visible assemblies. b) Photograph of the prototype. 1 – mains connection terminal, 2 – vacuum switch assembly, 3 – induction-dynamic drive, 4 – counter-current capacitor, 5 – commutation choke, 6 – resistor, 7 – thyristor unit, 8 – overcurrent relay, 9 – receiver connection terminal; 10 – internal surge arresters: 11 – diode, 12 – varistor; 13 – external surge arrester (varistor); 14 – control unit, 15 – energy measurement system, 16 – fuse, 17 – measuring shunt, 18 – energy meter, 19 – contactors unit

With the standardization rules [22], both base sizes are rated according to the needs and requirements of users, including the DC2 system. DCU-HM 3/1.6 in roof version for PZ or EZT is shown in Fig. 12 (horizontal installation).

DCU-HM 3/4.0 in deck version is mounted in the locomotive's HV cabinet (vertical installation). It has the same assemblies and functions but with larger cross-sections of the main current circuit elements.

The work of DCU-HM is managed by a specialized microcomputer (control unit 14 in Fig. 12a) with multifunctional proprietary software, which enables processing of data necessary for all the above-mentioned activities and functions. It is composed of a microprocessor controller, input/output interface, power supply, lock and drive power unit controllers, and a CAN network module for internal and external communication. All these units are integrated in a common casing and have mutual optical or electrical communication (as required). A control panel for external communication is placed on the housing. It is equipped with standardized, multi-channel electrical or fiber optic connections, enabling receiving and sending all necessary control (S1, S2, S3) or information signals (Fig. 11a). Standardization also includes all outputs of active or passive auxiliary contacts (multiplied by relays if necessary), indicating the position (state) of the switch, as well as a special connection for sending information via the CAN network. This enables visual signaling of the breaker status and other parameters required by the user. The controller has typical computer connectors and is equipped with an energy reader. Correct and reliable operation of DCU-HM under all current conditions requires high resistance to all types of internal and external electromagnetic interferences. In addition to known and typical methods of shielding, the breaker uses the principle of maximum use of fiber optic technology for digital communication between the breaker's controller and the assemblies. Analog electrical signals are used in necessary cases only. Each of the main switch assemblies is installed in a separate housing equipped with unified fiber optic and electrical connectors, cooperating with USW by means of unified WS and WE bundles, maintaining (if necessary) the principle of redundancy and operating according to the accepted principles of modularization and standardization of the DCU-HM circuit-breaker.

It was impossible to compare the new (DCU-HM) and old (MBOS) construction of the circuit breakers operating in the same circuits. Hence, the estimated parameters of DCU-HM were compared with the MBOS manufactured by GE Power Control (BWS circuit breakers). The oscillograms (see Fig. 13)

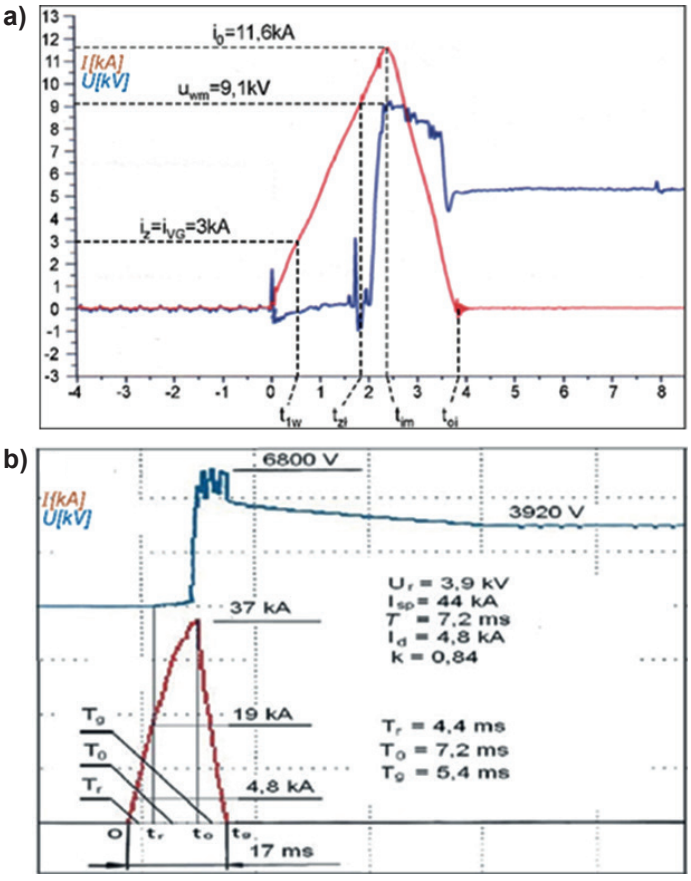

Fig. 13. Comparison of short-circuit current breaking performed by new (a) and (b) conventional construction of circuit breakers

show the switching off of the short-circuit current in slightly different circuits with unequal initial short-circuit current steepness. Moreover, there is a large difference in the settings of overcurrent releases of both circuit breakers, reaching approx. 50%. This may suggest that the limited current value recorded on the oscillogram for ultrafast circuit breaker is too low in relation to the circuit in which the BWS circuit breaker was tested. To explain this, it should be recalled that the ultra-fast breakers have an arc time in the vacuum chamber of approx. $T_a \leq 2$ ms.

After this time, from the moment the overcurrent release is tripped, the circuit current reaches a limited value i_o. Thus, if DCU-HM is used in the same circuit as the BWS breaker, i.e.:

$$\begin{aligned} &U_e = 3.9\ [\text{kV}], \quad I_{sp} \approx 44\ [\text{kA}], \quad \tau \approx 10\ [\text{ms}], \\ &di/dt \approx 4.4\ [\text{A}/\mu\text{s}], \quad I_t = 4800\ [\text{A}], \end{aligned} \tag{8}$$

it reduces the short-circuit current after the following time:

$$t = 4800/4.4 + 2000\ [\mu\text{s}] = 3090\ [\mu\text{s}], \tag{9}$$

and the current reaches the value below:

$$I = I_{sp}\left(1 - e^{-3.09/10}\right)[\text{A}] = 11.4\ [\text{kA}], \tag{10}$$

where: U_e – network voltage, I_{sp} – steady prospective short-circuit current, τ – time constant, $di/dt = s_i = I_{sp}/\tau$ – initial rate of short-circuit current rise, I_t – trip current.

Hence, the comparison of the selected parameters based on the appended oscillograms is possible, and it is presented in Table 1.

Table 1
Comparison of the effects of short-circuit breaking by DCU-HM and MBOS circuit breakers

No	Parameter name	P_D – symbol and value DCU-HM	P_M – symbol and value BWS	P_D/P_M*·100 [%]
1	Opening time	$T_o \leq 500$ µs	$T_o \leq 5$ ms	10%
2	Total break time	$T_w \leq 2$ ms	$T_w \leq 17$ ms	12%
3	Cut-off current at $s_i \approx 4{,}4$ A/µs	$i_o \leq 13.6$ kA	$i_o \leq 37$ kA	37%
4	Current limitation factor** at 4.4 A/µs	$C_o \approx 0.3$	$C_o \approx 0.84$	36%
5	Maximum magnetic energy	$E_m \leq 60$ kJ	$E_m \leq 616$ kJ	10%
6	Maximum Joule integral	$I^2t \leq 240$ kA^{2}s	$I^2t \leq 12250$ kA^{2}s	2%
7	Maximum arc energy	$E_a \leq 400$ J	$E_a \leq 700$ kJ	0.06%
8	Switching durability at I_{th} current C/O c.	$n_{et} \geq 30000 = n_{mV}$	over 10 times larger	1000%
9	Switching durability at I_{sp} current C/O c.	$n_{es} \geq 30000 = n_{mV}$	over 100 times larger	10000%

*P_D – DCU-HM parameter, P_M – equivalent parameter for MBOS.
**$C_o = i_o / I_{sp}$. I_t – trip current (preset).
C/O c. – close/open cycle (i.e. ON/OFF I_{th} or I_{sp}).
n_{mV} – VC mechanical durability.

With the capabilities listed in Table 1 and the work management described above, DCU-HM has the properties specified below, not available for MBOS.

— **When switching off a short-circuit**, one DCU-HM with high switching durability (Table 1) is equivalent to approximately 100 MBOS. At comparable prices, the investment costs over the lifetime of one DCU-HM is about 100 times lower. The estimated cost of a single short-circuit shutdown by DCU-HM is also about 100 times lower. Economic benefits cumulate at the user side.
— **Special systemic and electrical functions:**
  - two-sided limitation of overvoltage,
  - two levels of limitation for DC1 and DC2,
  - emergency arc protection,
  - protection of semiconductors with currents $I_{th} \geq 150$ A,
  - no interference with the recuperative braking process;
— **Special electronic and IT functions:**
  - measurement, registration, processing and archiving of data,
  - computerized event history preview,
  - computer diagnostics and adjustment of settings,
  - internal and external communication with users,
  - use of voltage and current measurement signals to measure energy with a certified meter.

This allows the DCU-HM switch to perform the special operational advantages:
— **Ultra-fast shutdown in a vacuum:**
  - low arc energy and contact wear,
  - short-circuit switching durability equal to mechanical life,
  - no critical currents, unnecessary protective zone and periodic service,
  - full environmental neutrality,
  - full selectivity at short circuits in relation to MBOS in substations.
— **Modular construction:**
  - variable spatial configuration,
  - adaptability to mounting spaces in different electric vehicles or substations,
  - roof, deck or sub-deck version possible.
— **Selective operation** with respect to substation breakers improves traffic run and passenger safety.

8. Conclusions

The paper presents the developed and patent pending ultra-fast hybrid switching systems for efficient and reliable protection of various medium and low voltage DC circuits with high magnetic energy. The excellent dynamic properties of USH result from unique construction of the inductive-dynamic drive that allows for decreasing the total break time below 2 ms. This is crucial to limit the harmful effects of quench and short circuits in railway systems. That is why USH has the performance capabilities not available for MBOS.

It could potentially be achieved due to the new technique of ultra-fast commutation of the current in a vacuum. Technical details concerning the structure and operation of USH (i.e. DCSS and DCU-HM) are given in [23, 24]. The new technique has been experimentally verified. It improves the effectiveness and reliability of anti-quench protection and railway systems protection. In fact, the reliability of the novel construction of the switching system is mainly limited by the durability of a vacuum chamber. Commercially available AC vacuum chambers, in practice, allow for building unipolar USH in the current range of up to 4–5 kA. For higher currents, parallel configurations are needed. The development potential of USH is high because they can be used in all fields of application of superconducting electromagnets (installed in CERN to protect LHC) and DC1, 2 electric traction systems. MBOS are still fully usable and have development potential in low power LVDC circuits [25].

Acknowledgements. The work on USH systems was co-financed by the European Organization for Nuclear Research CERN in Switzerland and by the National Centre for Research and Development in Poland.

- The program for the implementation of the DCSS family, designed to protect superconductive coils of electromagnets against quench, has been fully financed by the European Organization for Nuclear Research CERN according to the Framework Collaboration Agreement Reference KN 3093, Addendum No. 1–3, 2017–2020.
- The program for the implementation of the DCU-HM family, aimed at protecting the DC1 and DC2 rail systems, has been fully financed by the National Centre for Research and Development from the European Funds within the Smart Growth Operational Program, agreement No. POIR.04.01.04–00–0061/17–00, 2018–2021.

The funders had no role in the design of the study, in the collection, analyses or interpretation of data. Likewise, they did not participate in the writing of the manuscript or in the decision to publish the results.

The authors hereby declare no conflict of interest.

References

[1] A.N. Greenwood, P. Barkan, and W.C. Kracht, "HVDC vacuum circuit breakers", *IEEE Trans. Power App. Syst.* PAS-91(4), 1575–1588 (1972).

[2] C.W. Kimblin *et al.*, "Development of a current limiter using vacuum arc commutation", EPRI EL-393 Research Proj. 564–1, USA, 1977.

[3] T. Senda, T. Tamagawa, K. Higuchi, T. Horiuchi, and S. Yanabu, "Development of HVDC circuit breaker based on hybrid interruption scheme", *IEEE Trans. Power App. Syst*. PAS-103(3), 545–552 (1984).

[4] M. Bartosik, "Progress in DC breaking", *Proc. 8th Int. Conf. Switching Arc Phenomena SAP 1997*, *part 2*, Lodz, Poland, 1997, pp. 29–41.

[5] M. Bartosik, R. Lasota, and F.Wójcik, "New generation of D.C. circuit breakers", *Proc. 3rd Int. Conf. on Electrical Contacts*, *Arcs*, *Apparatus and Appl. (IC-ECAAA)*, Xian, China, 1997, pp. 349–353.

[6] A. Daibo, Y. Niwa, N. Asari, W. Sakaguchi, K. Takimoto, K. Kanaya, and T. Ishiguro, "High-speed current interruption performance of hybrid DCCB for HVDC transmission system", *IEEE J. Ind. Appl.* 8(5), 835–842 (2019).

[7] N. Xia, J. Zou, D. Liang, Y. Gao, Z. Huang, and Y. Wang, "Investigations on the safe stroke of mechanical HVDC vacuum circuit breaker", *J. Eng. (IET)* 16, 3022–3025 (2019).

[8] R. Rodrigues, Y. Du, A. Antoniazzi, and P. Cairoli, "A Review of Solid-State Circuit Breakers", *IEEE Trans. Power Electron.* 36(1), 364–377, (2021).

[9] M. Wilson, "Superconducting Magnets for Accelerators", CAS, 2006. [Online]. Available: https://cas.web.cern.ch/sites/cas.web.cern.ch/files/lectures/zakopane-2006/wilson-lect.pdf

[10] F. Wójcik, "Ultra-fast shutdown of DC power circuits", *Sc. Bull.* 1071, TUL, Sc. Papers 396. Habilitation thesis. Lodz, Poland, 2010, [in Polish].

[11] PN-EN 50123-1. Railway applications. Fixed installations. DC switchgear. General requirements. *(PL/EU standard)*.

[12] M. Bartosik, R. Lasota, and F. Wójcik, "Direct current-limiting vacuum circuit breaker", *Proc. 12th Symp. "Electrical Phenomena in Vacuum" ZEP-91*, *Sc. Fasc. Elektryka* 39, Tech. Univ. of Poznan, Poland, 1991, pp. 21–24.

[13] M. Bartosik, R. Lasota, and F. Wójcik, "Arcless D.C. hybrid circuit breaker", *Proc. 8th Int. Conf. Switching Arc Phenomena SAP-97*, Lodz, Poland, 1997, pp. 115–119.

[14] M. Bartosik, R. Lasota, and F. Wójcik, "New type of DC vacuum circuit-breakers for locomotives", *Proc. 9th Int. Conf. Switching Arc Phenomena SAP-2000(1)*, *Conf. Mat.* Lodz, Poland, 2001, pp. 49–53.

[15] M. Bartosik, R. Lasota, and F. Wójcik, "Ultra-High-Speed D.C. Hybrid Circuit-Breakers of DCNT Type for Substations of Urban and Mine Traction", *Proc. of the 10th Int. Conf. Switching Arc Phenomena*, Lodz, Poland, 2005, pp. 360–364.

[16] M. Bartosik, P. Borkowski, E. Raj, and F. Wójcik, "The New Family of Low-Voltage, Hyper-Speed Arcless, Hybrid, DC Circuit Breakers for Urban Traction Vehicles and Related Industrial Applications", *IEEE Trans. Power Del.* 34(1), 251–259 (2019).

[17] Ch. Peng, A. Huang, I. Husain, B. Lequesne, and R. Briggs, "Drive circuits for ultra-fast and reliable actuation of Thomson coil actuators used in hybrid AC and DC circuit breakers", *IEEE Appl. Power Electronics Conf. and Exp. (APEC)*, 2016, pp. 2927–2934.

[18] K. Krasuski, P. Berowski, A. Dzierżyński, A. Hejduk, S. Kozak, and H. Sibilski, "Analysis of arc in a vacuum chamber with an AMF", *Proc. Electrotech. Inst.* 269, 91–99 (2015).

[19] P.G. Slade, *The Vacuum Interrupter Theory*, *Design and Application*, CRC Press, 2007.

[20] "Vacuum interrupters", Eaton Holec Cath. No. 3.9.1.

[21] T. Maciołek, M. Lewandowski, A. Szeląg, and M. Steczek, "Influence of contact gaps on the conditions of vehicles supply and wear and tear of catenary wires in a 3 kV DC traction system", *Bull. Pol. Acad. Sci. Tech. Sci.* 68(4), 759–768 (2020).

[22] The applicable standards: PN-EN 50121–3-2, PN-EN 50123-1, PN-EN 50123-2, PN EN 50123-5, PN-EN 50124-1, PN-EN 50153, PN-EN 50155, PN-EN 50163, PN-EN 60068-1 (also: 60068-2-1, 60068-2-2, 60068-2-52), PN-EN 60077-1 (also: 60077-2), PN-EN 60077-3, PN-EN 60529, UIC Charter 550/1997.

[23] M. Bartosik, P. Borkowski, and F. Wójcik, "Ultra-fast hybrid, vacuum-semiconductor switch to reduce the effects of quench in DC-powered superconducting induction circuits with high magnetic energies", Polish Patent Office, P.429439, (DCSS), granted (2021).

[24] M. Bartosik, P. Borkowski, A. Jeske, Ł. Nowak, and F. Wójcik, "Ultra-fast DC hybrid circuit breaker designed especially for railway traction", Polish Patent Office, P.429285, (DCU-HM), granted (2021).

[25] Ł. Kolimas, S. Łapczynski, M. Szulborski, and M. Świetlik, "Low voltage modular circuit breakers: FEM employment for modelling of arc chambers", *Bull. Pol. Acad. Sci. Tech. Sci.* 68(1), 61–70 (2020).

List of abbreviations used in the article

AC – alternating current
AMF – axial magnetic field
APSU – auxiliary power supply unit
BSM – bidirectional semiconductor module
DC – direct current
DC1 or DC2 – systems of railway traction of 3 kV or 1.5 kV voltage
DCPS – direct current power supply
DCS – ultra-fast DC hybrid switch
DCSS – direct current switching system
DCU-HM – direct current ultra-fast hybrid modular switch
DP/AP – overcurrent relay
EES – energy extraction system
EW – electric vehicle.
EZT – electric traction unit
GP – counter-current generator
HV, MV or LV – high, medium or low voltage
HVDC, MVDC or LVDC – high, medium or low voltage DC systems
IDD – induction-dynamic drive
L – locomotive
LHC – Large Hadron Collider
MBOS – magnetic blow-out switches
PZ – combined train
QDS – quench detection system
RD – dump resistor
SE or SM – superconductive electromagnet or magnet
SS v.1 – shutdown algorithm sequence for forced commutation
SS v.2 – shutdown algorithm sequence for natural commutation
U DCCB – ultra-fast DC circuit-breaker
U DCCB – ultra-fast DC circuit-breakers
USH – ultra-fast hybrid switching systems
v.1 – variants of DCS or DCSS with forced commutation
v.2 – variants of DCS or DCSS with natural commutation
VC – vacuum chamber
Other symbols were defined in the text.